Supplementary material: Growth of barchan dunes of bidispersed granular mixtures

Carlos Azael Alvarez,[a] Fernando David Cúñez, and Erick M. Franklin[b]

School of Mechanical Engineering, UNICAMP - University of Campinas, Rua Mendeleyev, 200, Campinas, SP, Brazil

(Dated: 7 May 2021)

[a]Also at Department of Atmospheric and Oceanic Sciences, University of California, Los Angeles, Los Angeles, CA 90095-1565, USA

[b]Electronic mail: erick.franklin@unicamp.br; Corresponding author

Introduction

This supplementary material presents the layout of the experimental device, microscopy images of the used grains, snapshots of barchans of different grain types, additional graphics of grain trajectories, and movies showing examples bidispersed barchan evolutions. For the latter, we present top view movies for different densities, different sizes, and different densities and sizes, and a side view movie for different grain sizes. All movies have been sped up by 2x. We note that individual images and movies used in the manuscript are available on Mendeley Data (https://data.mendeley.com/datasets/z42c97sw4c).

The experiments described in the paper were conducted in a water channel of transparent material, for which the layout is shown in Fig. 1. With the channel previously filled with water, controlled grains were poured inside, forming conical piles consisting of bidispersed grains that were afterward deformed into a barchan dune by imposing a water flow.

We used two cameras of complementary metal-oxide-semiconductor (CMOS) type. One, placed above the channel, acquired top view images of the bedform while the other, placed horizontally, acquired side-view images. The resolution of both cameras was of 1920 px $\times$ 1080 px at 60 Hz and they were mounted on a traveling system. The regions of interest (ROI) were set to 1920 px $\times$ 941 px and 1280 px $\times$ 241 px for the top and lateral cameras, respectively, and the frequency to 60 Hz. We used lenses of 18 - 140 mm and 18 - 105 mm focal distances mounted on the top and lateral cameras, respectively, and lamps of light-emitting diode (LED) were branched to a continuous-current source to provide the necessary light while avoiding beating. The conversion from px to a physical system of units was made based on images of a scale placed in the channel previously filled with water. The acquired images were afterward processed by numerical scripts written in the course of this work.

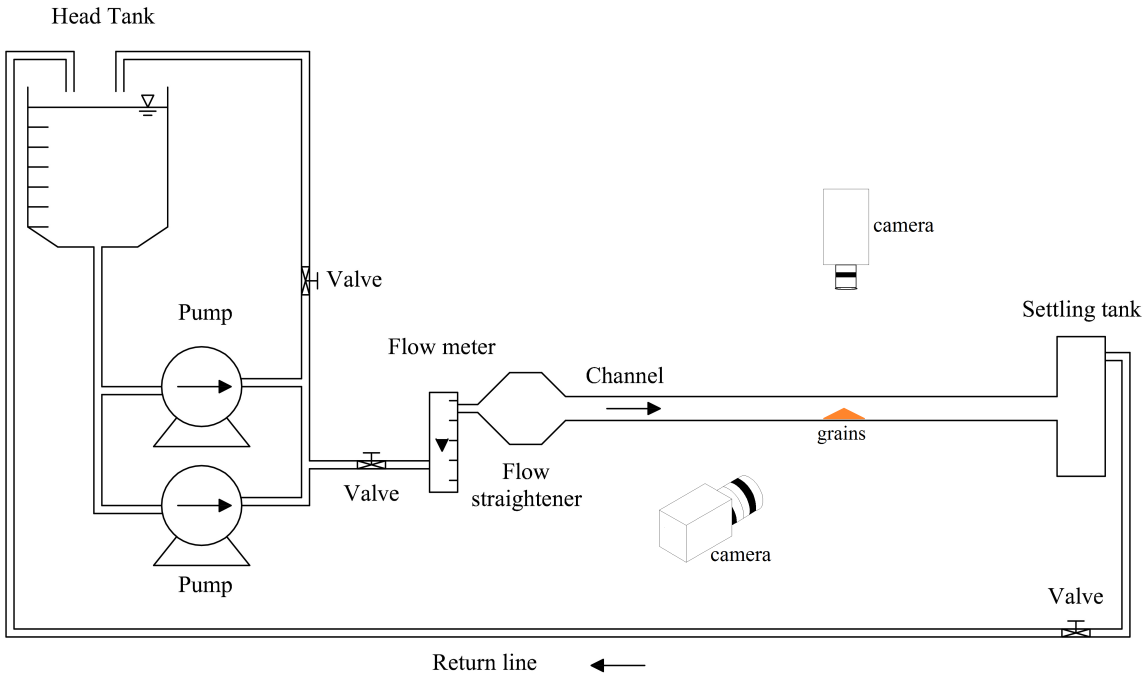

FIG. 1. Layout of the experimental setup.

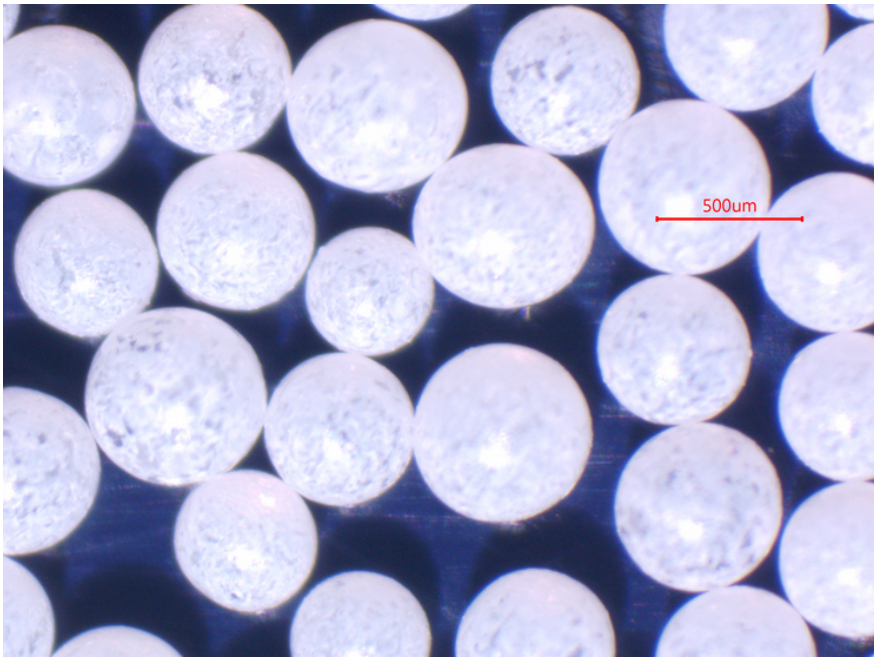

FIG. 2. Microscopy image for the 0.40 mm $\leq d \leq$ 0.60 mm round glass beads of white color.

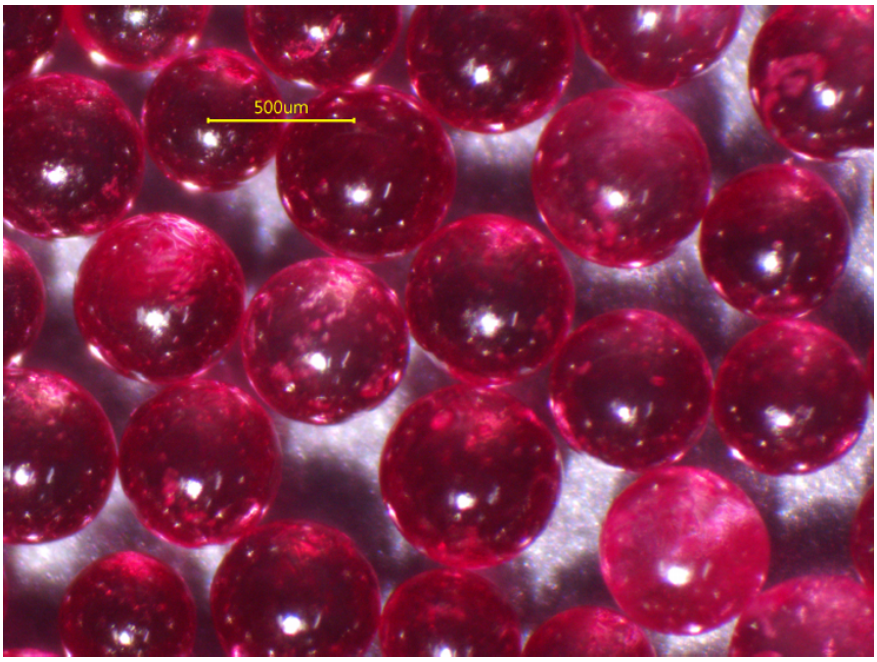

FIG. 3. Microscopy image for the 0.40 mm $\leq d \leq$ 0.60 mm round glass beads of red color.

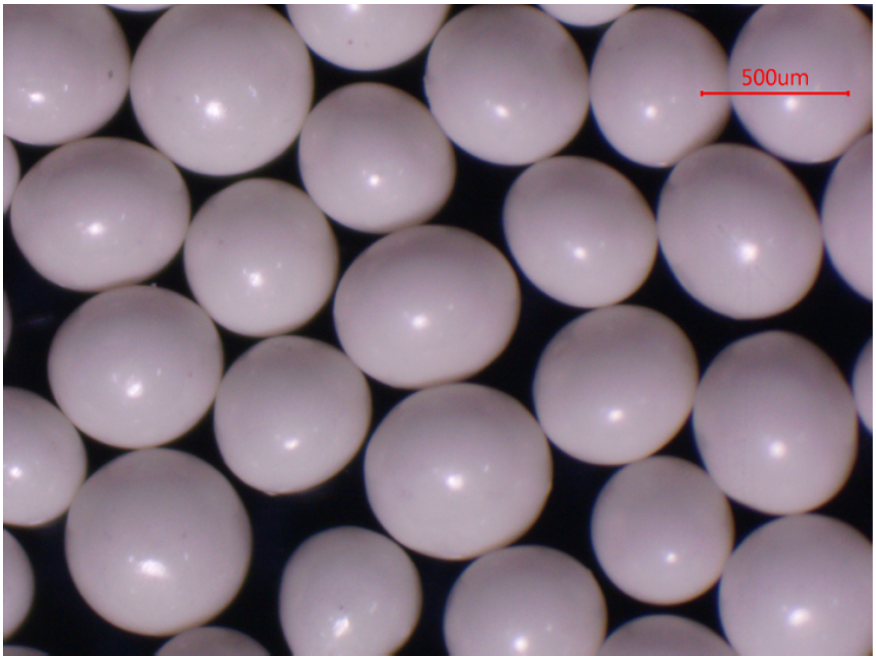

FIG. 4. Microscopy image for the 0.40 mm $\leq d \leq$ 0.60 mm round zirconia beads.

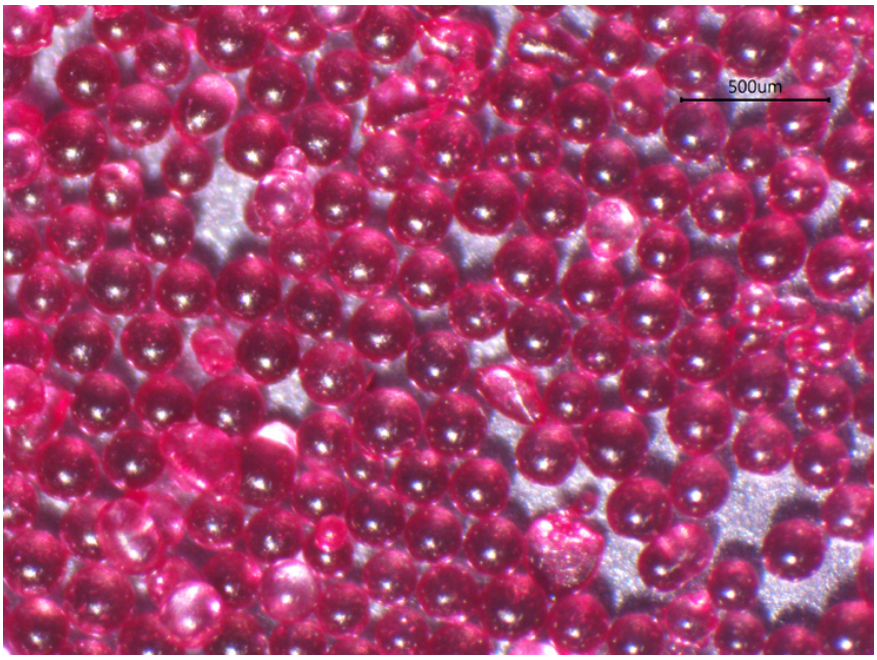

FIG. 5. Microscopy image for the 0.15 mm $\leq d \leq$ 0.25 mm round glass beads of red color.

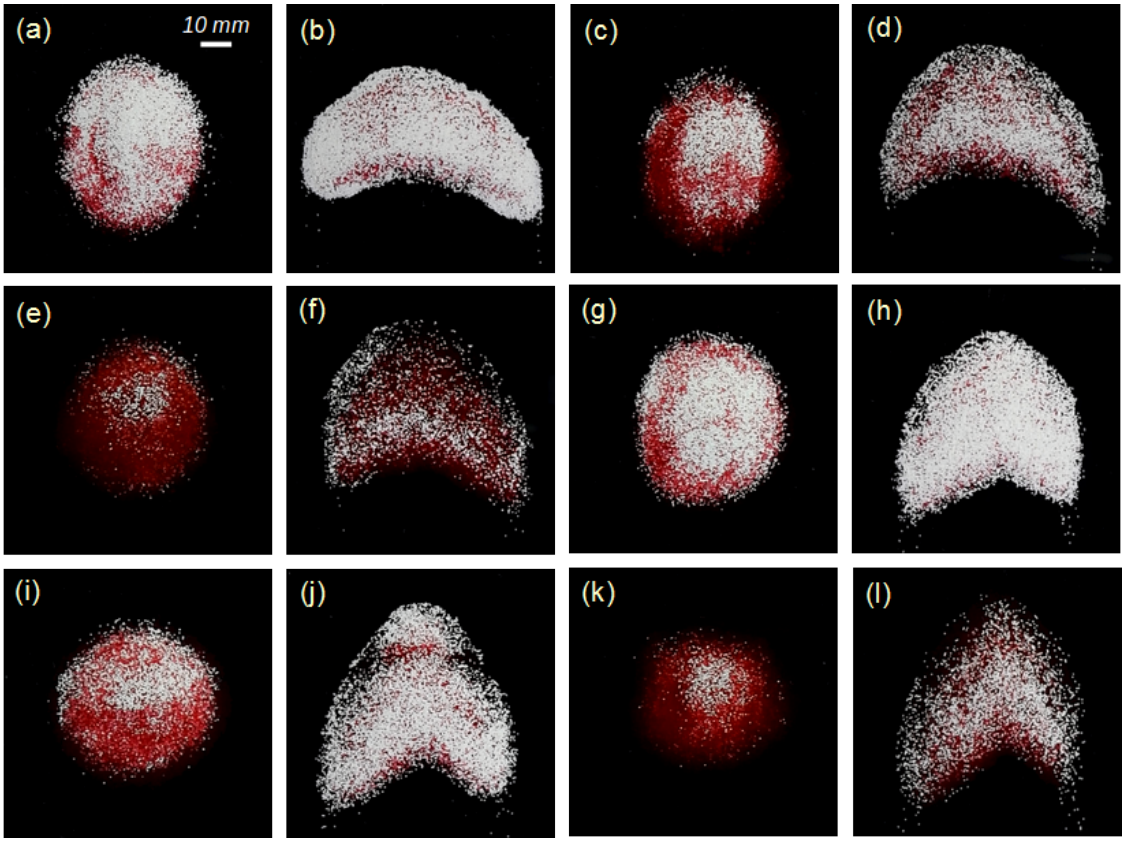

FIG. 6. Top view of the initial pile and barchan dune for dunes of different densities and same diameter. Figures (a) and (b) to (k) and (l), by pairs, correspond to the initial pile and barchan, respectively, of cases a to f.

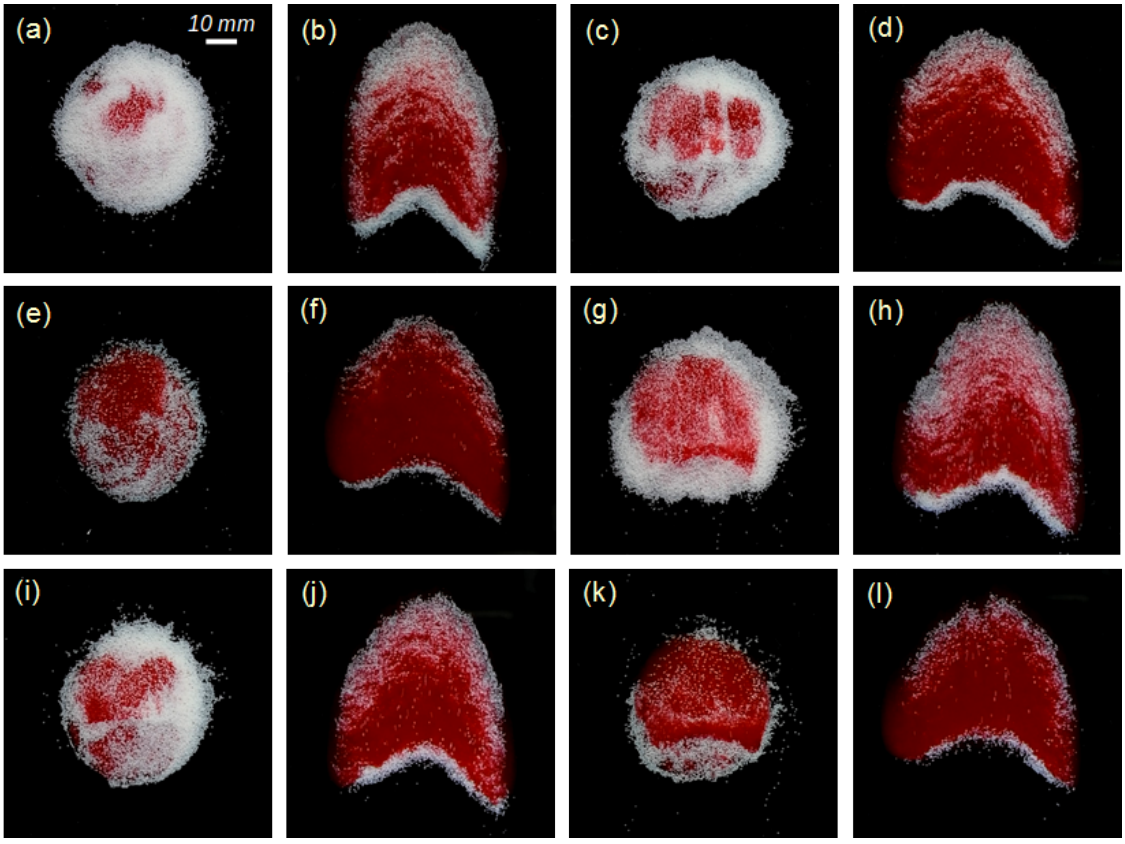

FIG. 7. Top view of the initial pile and barchan dune for dunes of same density and different diameters. Figures (a) and (b) to (k) and (l), by pairs, correspond to the initial pile and barchan, respectively, of cases g to l.

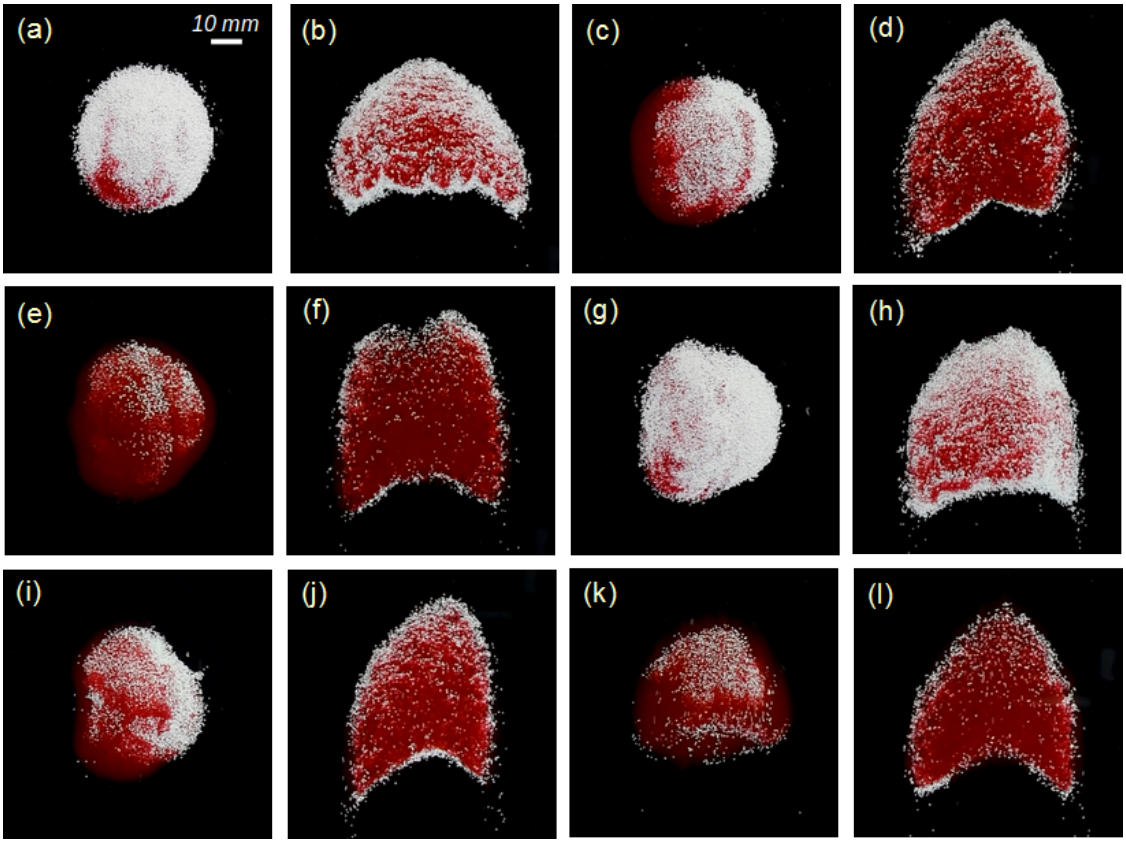

FIG. 8. Top view of the initial pile and barchan dune for dunes of different densities and diameters. Figures (a) and (b) to (k) and (l), by pairs, correspond to the initial pile and barchan, respectively, of cases m to r.

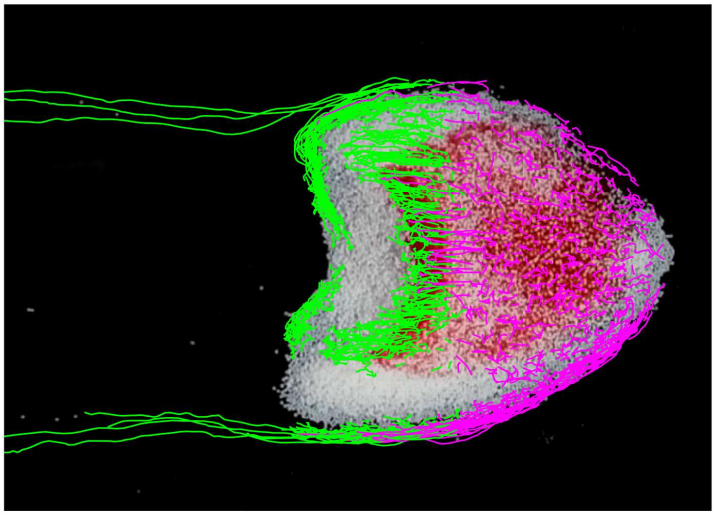

(a)

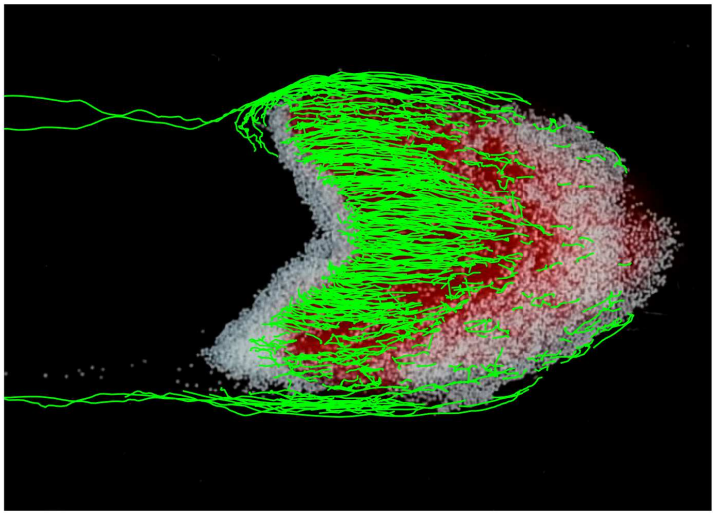

(b)

FIG. 9. Trajectories of larger grains of case g, for two different intervals: Figure (a), from t = 25 to 65 s, when the stripe was still present, and Figure (b), from t = 170 to 210 s, when it had already vanished. In Figure (a), green lines correspond to grains that started moving in positions downstream the transverse stripe, while magenta lines correspond to those that started moving in position upstream the stripe. In the figure, flow is from right to left

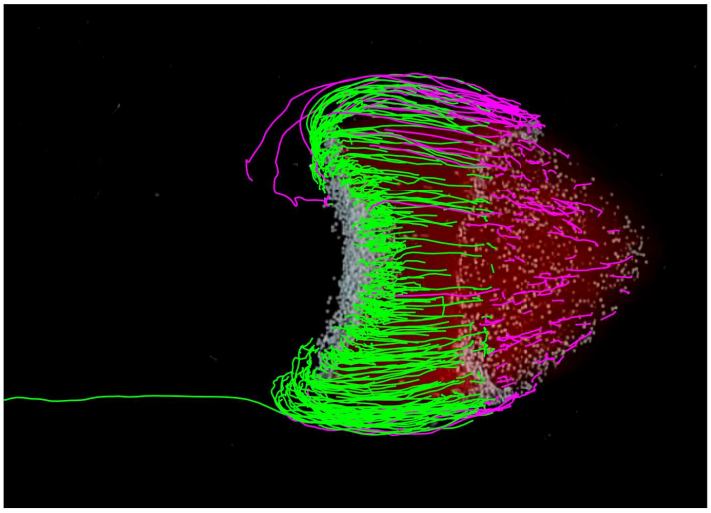

(a)

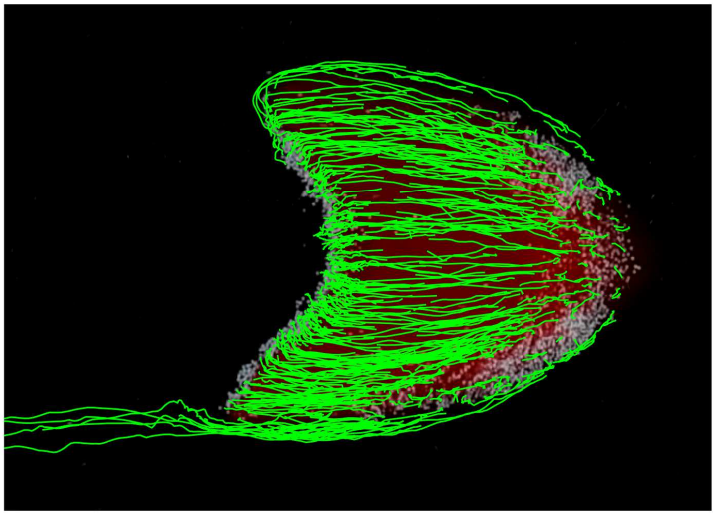

(b)

FIG. 10. Trajectories of larger grains of case i, for two different intervals: Figure (a), from t = 40 to 80 s, when the stripe was still present, and Figure (b), from t = 150 to 190 s, when it had already vanished. In Figure (a), green lines correspond to grains that started moving in positions downstream the transverse stripe, while magenta lines correspond to those that started moving in position upstream the stripe. In the figure, flow is from right to left

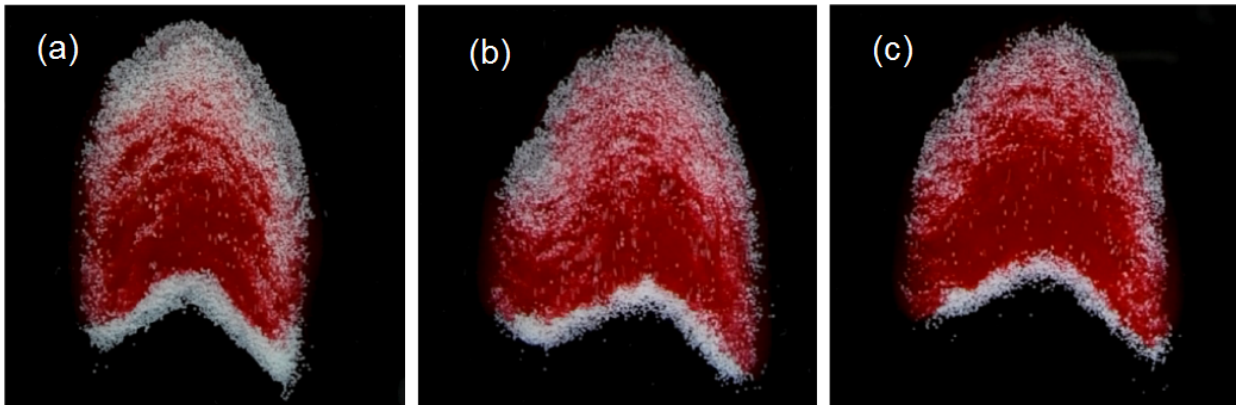

FIG. 11. Examples of oblique stripes observed on some dunes. (a) Case g at t = 240 s. (b) Case j at t = 120 s. (c) Case k at t = 130 s.

TABLE I. Values of Re_* and θ for each species and flow conditions.

Species	Re	Re_*	θ
S_1	1.47×10^4	8	0.02
S_1	1.82×10^4	10	0.03
S_2	1.47×10^4	8	0.04
S_2	1.82×10^4	10	0.06
S_3	1.47×10^4	3	0.10
S_3	1.82×10^4	4	0.14

TABLE II. Arithmetic mean of the wavelengths of oblique stripes, λ for cases g, h, j and k.

Case	λ	λ/d
$\cdots$	(mm)	$\cdots$
g	2.4	13
h	3.1	16
j	2.5	13
k	2.7	14

TABLE III. Final instant of the initial phase of the diffusion process, t_i, and of the test run, t_f, normalized by t_c, for each tested case. t_c is the characteristic time for the displacement of barchans (computed as the dune length divided by its celerity, as presented in Alvarez and Franklin, Phys. Rev. E, 96, 062906, 2017).

case	t_i/t_c	t_f/t_c
a	1.0	8.0
b	1.4	10.1
c	1.6	8.0
d	1.2	4.3
e	1.5	3.4
f	1.8	3.5
g	2.5	5.0
h	5.0	12.0
i	1.7	7.4
j	2.0	9.6
k	4.0	9.5
l	3.0	16.5
m	7.2	12.7
n	4.3	13.8
o	3.6	14.4
p	2.4	4.1
q	2.8	9.6
r	4.4	11.7

TABLE IV. Average distances traveled by the species S_2 upstream and downstream the transverse stripe, Δ_{up} and Δ_{down}, respectively, the corresponding average velocities, $\overline{V}_{up}$ and $\overline{V}_{down}$, respectively, and average distances traveled by species S_2 and corresponding velocities after the transverse stripe has disappeared, Δ_{tot} and $\overline{V}_{tot}$, respectively, for cases g, h, and i. Upstream and downstream averages were computed when the stripe was in the middle of the stoss face. Distances are normalized by the grain diameter and velocities by the shear velocity on the channel wall.

Case	Δ_{up}/d	Δ_{down}/d	Δ_{tot}/d	$\overline{V}_{up}/u_*$	$\overline{V}_{down}/u_*$	$\overline{V}_{tot}/u_*$
g	16.6	19.8	21.4	0.20	0.52	0.51
h	9.4	14.0	19.9	0.25	0.60	0.67
i	11.8	13.4	17.4	0.31	0.67	0.66